My Comments to referee 1:

Q:In general, the paper misses from a formal uncertainty analysis of measured and derived parameters. Also, uncertainties are missing in all plots. Please correct this and add more formal error discussion. For example, in Figure 7 of the paper we can see differences between the dust and non-dust cases, but what is the real difference within uncertainties?
A:In figure 7 the standard deviation of the average of the Sahara and Non_Sahara data has been added. It is obvious that a significant difference between the two datasets exists. Doing this I realized that I plotted the wrong average for the Sahara aerosol. Instead of copying the average I copied the line above, which was the last measurement of the Sahara aerosol

Q:Specific comments
Page 1, line 29: please check the extra comma in the text:
A: has been corrected

Q: Page 2, line 4: add references after "larger particles"
A: I have added a short discussion of the average residence time of the particles, including a reference

Q: Page 2, line 12: E should be replaced by S, I guess
A: This was a mistake, thank you for pointing it out.

Q: Page 2, line 30: please check the formula since I think you missed a minus sign before the angstrom exponent; if I am right, then check the following discussion.
A: There are two ways to use the Angström formula: $\sigma(\lambda) = \sigma(\lambda_0)\cdot(\lambda/\lambda_0)^{\alpha}$ or $\sigma(\lambda) = \sigma(\lambda_0)\cdot(\lambda/\lambda_0)^{-\alpha}$
I have used the first possibility, which historically was used earlier. It is used consistently in the paper.

Q: Page 3, line 5: I do not like the expression "usual aerosol", please be more specific (pollution aerosols, fine aerosols?).
A: I have replaced "usual aerosol" by "non-Sahara aerosol"

Q: Page 3 line 5; I would replace with "is a sign for desert aerosol particles" with "it is a sign for large aerosols, as desert dust" or similar
A: I have changed it to "an aerosol containing larger particles, in this study mainly desert particles"

Q: Page 3, line 25: how the extrapolation is done?
A: The method is described in detail in the reference (Horvath, 2015) given in the paper under discussion. Since this reference is a 10 page paper I can only give a short description: Analyzing a large set of scattering functions of both spherical and non-spherical particles it was found, that it is possible to predict the shape of the scattering function for a few degrees ahead if the shape of the curve is known up to the point, where the extrapolation starts. Since only 5 degrees are missing this can be done quite accurately.

Q: Page 4, line 5: you refer to "all the instruments", which instruments? Please describe clearly the instruments used. I am also a bit confused by the fluxes. A flux of aspiration for the custom made nephelometer is specified in the previous page, while here there is reference to a different flow rate. What is this for?
Q: The SLOPE study mainly was intended to determine the vertical structure of the aerosol by remote sensing instruments. So the main instruments were sun and sky photometers and an airplane. Obviously ground based instruments were also used. At the Albergue Universitaria, several instruments were operated. It is a standard practice to connect these instruments to a central sampling

port. This is a vertical tube extending above the roof, through which air is sucked into the laboratory by a blower. The flow rate is chosen such that as little as possible disturbances of the aerosol take place, thus it can be assumed that the instruments sample undisturbed outside air. I have listed the other instruments, although they are irrelevant for this study.

Q: Page 4, line 12: again there is the expression “usual aerosol” to modify
A: Has been replaced by non-Sahara aerosol

Q: Page 4, line 19-22: the integrated nephelometer mentioned in this paragraph was not introduced before. Please, again, clearly indicate the used instruments and their configuration.
A: I have listed the other instruments although they are irrelevant for this study.

Q: Moreover, what about the integrating nephelometer (model, data treatment, uncertainties)?
A: I have added three lines on the Integrating Nephelometer and a reference to the NOAA site. (Since NOAA uses this instrument since more than 20 years at their baseline station, the instrument is thoroughly tested and competent instructions on calibration and evaluation can be found on the site)

Q: The data shown in Figure 5 for example are corrected for truncation, and if yes, how?
A: In figure 5 no truncation procedure is needed to apply. The calibration of the Integrating Nephelometer is done according to the NOAA instructions and compared to the integrated volume scattering function of the polar nephelometer, which should be identical.

The effect of truncation is shown in Figure 9 and I have added an explanation how the signals BsbG and BsG are obtained, when using the measured volume scattering function.

Q: And what about the uncertainty?
A: This question is difficult to answer. Under laboratory conditions i.e. when a constant aerosol is produced e.g. by a constant output atomizer, the Integrating Nephelometer measures a signal which is constant as long as the atomizer is in operation. Similarily the polar nephelometer measures identical volume scattering functions, which, when plotted on top of each other are one line. So the uncertainty of both instruments is 2% or even better. BUT the atmosphere is not laboratory with a constant aerosol, especially at the site in the Sierra Nevada with a layered aerosol. This can best be seen in Figure 5. The continuous line is the scattering coefficient of the aerosol (if the aerosol were constant the instrument would produce a horizontal line). So the aerosol is variable and the instruments measure this variable aerosol with very little uncertainty. The variability of the aerosol can best be seen in figure 7 and Table 2. For the aerosols classified as Sahara, the phase function at 90° e.g. is 0.35 sr^{-1} with a standard deviation of 0.04sr^{-1} or 11%. But this variability is not caused by an imprecise instrument, but by an aerosol which just is not constant.

Q: Section 5: together with the asymmetry factor is also possible to retrieve the lidar ratio at the used wavelength of 532 nm? If yes, I would suggest to do it. The lidar ratio is a useful parameter to provide as output.
A: The lidar ratio is defined as the extinction coefficient divided by volume scattering coefficient at 180°, or 4π /([P(180°) .ω], with ω the single scattering albedo. I have used an average value for ω and the value for the lidar ratio is listed in table 2.

Angular Scattering of the Sahara Dust Aerosol

Helmuth Horvath[1], Lucas Alados Arboledas[2,3], Francisco Jose Olmo Reyes[2,3]

[1]University of Vienna, Faculty of Physics, Aerosol Physics and Environmental Physics, A-1090 Vienna, Austria
[2]University of Granada, Department of Applied Physics, E-18071 Granada, Spain
3Andalusian Institute for Earth System Research (IISTA-CEAMA), Granada, Spain

Correspondence to: Helmuth Horvath (Helmuth.Horvath@univie.ac.at)

Abstract. Soil erosion aerosols can be transported considerable distances, the Sahara is one of the major sources on the world. In June 2016 the volume scattering function of the atmospheric aerosol has been determined in the Sierra Nevada, Spain, at an altitude of 2500 m. Measurements were performed with a polar nephelometer permitting measurements between scattering angles of 5° to 175°. The values at the missing angles could be estimated to a high accuracy, using the shape of the scattering function adjacent to the missing angles, thus a complete volume scattering function was available. During the measuring period intrusions of long range transported Sahara aerosol happened several times. The classification of the aerosol was done by back trajectories and by the Angström exponent of the wavelength dependent scattering coefficient, which was determined by a three wavelength Integrating Nephelometer. The phase function of the Sahara aerosol had a stronger forward scattering, ~~more side scattering~~ and less backscattering compared to the non-Sahara~~usual~~ aerosol, which is in agreement with other findings for irregular particles. The asymmetry parameter of the phase function is the best characteristic to distinguish Sahara Aerosol from non-Sahara aerosol. In this study the asymmetry parameter for the Sahara aerosol was larger than 0.65, whereas the non-Sahara aerosol had an asymmetry parameter below 0.6. A comparison with measurements performed with long range transported Gobi Desert aerosols observed in Kyoto, Japan, showed very similar results.

1. Introduction

Deserts are a major source of aerosol particles. On a global scale the desert aerosol contributes 60–1800Tg/y of the total yearly aerosol production of 2900–4000 Tg (Jaenicke, 1988). Junge (1979) estimates the global source strength of deserts as 260 to 400 Tg/y, with the Sahara contributing 60 to 200 Tg/y. IPCC (2001) estimates the yearly mineral dust emissions as 1000 to 3000 Tg/y, amounting to 1/3 to ½ of the global emissions. In contrary to most of the other particles present in the atmosphere, desert aerosol particles are produced from minerals by mechanical processes, which obviously lead to irregular shaped particles. This is documented by innumerous electron micrograph studies (see e.g. Falkovich et al. 2001, Iwasaka et al., 2003~~,~~ Kandler et al, 2006). Among many other effects, the desert aerosol is expected to have an influence on the radiative balance, see e.g. Obregón (2014), Valencuela et al. (2012), Antòn et al. (2014).

My comments to referee 2

Q: General comments
- The introduction is extremely short. It should at least include information (scope instruments involved, locations, etc.) on the SLOPE campaign to which the measurements belong.
A: The instruments are described in the revised version as well as the SLOPE campaign. The location (Albergue Universitario of the University of Granada, located in the Sierra Nevada at an elevation of 2505 m a.s.l. Its coordinates are 37° 5' 43.72"N, 3° 23' 12.57"W) is already described on page 4 of the paper under discussion.

Q: Also some annual statistic of Sahara sand dust storm over southern Europe would be appreciated.
A: I have added the total days and the total number of Sahara dust events, from May to September 2016, as well as a reference in a footnote.
Q: - Information and proper references are provided for the custom made polar nephelometer but no information at all is given for the (commercial?) integrating nephelometer. Please, include in section 3 (instrumentS and method) basic information for the integrating nephelometer.
A: I have added three lines on the Integrating Nephelometer and a reference to the NOAA site. (Since NOAA uses this instrument since more than 20 years at their baseline stations, the instrument is thoroughly tested and competent instructions on calibration and evaluation can be found on the site)

Q:That would help in understanding e.g. the text in page 6, lines 5-10. How are BbsG and BsG defined ?
A: A definition is given towards the end of section 5.

Q: - As mentioned in the text the measurements are performed in a certain time period but not continuously.
A: First an explanation for the discontinuity of the measurements: Computer failure (I/O error) stopped the measurement and it had to be started manually. Since I stayed at Granada and was brought to the measuring site, no data could be obtained until I returned to the site. From June 17 to 24, 2016 I had to be at the University of Vienna and no measurements could be performed.
The Integrating Nephleometer less frequently failed to work.

Q: Please, provide a table with detailed information on the July 2016 Sierra Nevada campaign: instruments (nephelometer/integrating nephelometer), dates, sample time.
A: This actually can be seen in figure 5 of the paper under discussion. The red line gives the data of the Integrating Nephelometer, one can see a few periods of failure. The black dots are the measurements of the polar nephelometer, So I do not think it is not necessary to add an extra table, which does not give more information.

Q: It would also be interesting to combine the time table of the measurements with the information on the back trajectories from NOAA (current Table 1).
A: This actually was already done in figure 4: at the top of the figure the classifications can be found.

Q: Section 4.
- Results: How are period 1, 2 and, 3 defined?

A: The choice of the periods was accidentally, due to failure and absence (see above). Unexpectedly in these periods different aerosols dominated.

Q:- According to Figure 4 it seems like simultaneous measurements with the integrating and polar nephelometer are obtained. However, in Figure 5 the measured integrated volume scattering functions are obtained in narrower time periods. Please, clarify.
A: Please note that in figure 4 the scale has two breaks in the x-axis, so periods, where no measurements with the polar nephelomenter could be performed are not shown. I have used this representation in order to show more details.

Q:Minor comments:
- Page 3, first paragraph, 2nd line: “alpha <-1” should be “alpha < 0”.
A: Has been corrected
Q:- Page 3, last paragraph, second line: “Using data given by given by” should be “given by”
A: Has been corrected
Q:- Page 5, line 29: “In figure 5..”do you mean in Figure 4?
A:You are right this has been a mistake and is corrected.

Angular Scattering of the Sahara Dust Aerosol

Helmuth Horvath[1], Lucas Alados Arboledas[2,3], Francisco Jose Olmo Reyes[2,3]

[1]University of Vienna, Faculty of Physics, Aerosol Physics and Environmental Physics, A-1090 Vienna, Austria
[2]University of Granada, Department of Applied Physics, E-18071 Granada, Spain
3Andalusian Institute for Earth System Research (IISTA-CEAMA), Granada, Spain

Correspondence to: Helmuth Horvath (Helmuth.Horvath@univie.ac.at)

Abstract. Soil erosion aerosols can be transported considerable distances, the Sahara is one of the major sources on the world. In June 2016 the volume scattering function of the atmospheric aerosol has been determined in the Sierra Nevada, Spain, at an altitude of 2500 m. Measurements were performed with a polar nephelometer permitting measurements between scattering angles of 5° to 175°. The values at the missing angles could be estimated to a high accuracy, using the shape of the scattering function adjacent to the missing angles, thus a complete volume scattering function was available. During the measuring period intrusions of long range transported Sahara aerosol happened several times. The classification of the aerosol was done by back trajectories and by the Angström exponent of the wavelength dependent scattering coefficient, which was determined by a three wavelength Integrating Nephelometer. The phase function of the Sahara aerosol had a stronger forward scattering, ~~more side scattering~~ and less backscattering compared to the non-Sahara~~usual~~ aerosol, which is in agreement with other findings for irregular particles. The asymmetry parameter of the phase function is the best characteristic to distinguish Sahara Aerosol from non-Sahara aerosol. In this study the asymmetry parameter for the Sahara aerosol was larger than 0.65, whereas the non-Sahara aerosol had an asymmetry parameter below 0.6. A comparison with measurements performed with long range transported Gobi Desert aerosols observed in Kyoto, Japan, showed very similar results.

1. Introduction

Deserts are a major source of aerosol particles. On a global scale the desert aerosol contributes 60–1800Tg/y of the total yearly aerosol production of 2900–4000 Tg (Jaenicke, 1988). Junge (1979) estimates the global source strength of deserts as 260 to 400 Tg/y, with the Sahara contributing 60 to 200 Tg/y. IPCC (2001) estimates the yearly mineral dust emissions as 1000 to 3000 Tg/y, amounting to 1/3 to ½ of the global emissions. In contrary to most of the other particles present in the atmosphere, desert aerosol particles are produced from minerals by mechanical processes, which obviously lead to irregular shaped particles. This is documented by innumerous electron micrograph studies (see e.g. Falkovich et al. 2001, Iwasaka et al., 2003~~,~~ Kandler et al, 2006). Among many other effects, the desert aerosol is expected to have an influence on the radiative balance, see e.g. Obregón (2014), Valencuela et al. (2012), Antòn et al. (2014).

The mechanical production of particles results in particle sizes usually larger than 1 µm. Mean sizes range up to 10µm (Kontratyev et al. (2006), Alfaro et al. (2003), Cheng et al. (2005), Xin et al. (2005), Alfaro & Gomez, (2001), Falkovich et al., (2001)), and during atmospheric transport the size distribution is modified, mainly due to the shorter life time ~~settling of~~ of larger particles: The average residence time in the troposphere is estimated as 10 days for 1 µm particles and 3 days for 10 µm particles. (Jaenicke, 1988)

Since the dust particles have an irregular shape, their scattering properties are difficult to model, but their scattering properties are urgently needed to estimate the effect on climate. Below we report measurements of the volume scattering function of the Sahara aerosol transported to the Iberian Peninsula, which were performed during several dust outbreaks.

2 Definitions, units, and nomenclature

The volume scattering function $\gamma(\theta)$ of the aerosol is defined as follows, see figure 1: Let a volume dV of aerosol be illuminated by radiation having a flux density S. The light flux $d\Phi$ scattered into a solid angle $d\omega$ at the scattering angle θ is obtained as

$d\Phi = E\ S.\ \gamma(\theta)\ .\ d\omega\ .\ dV.$ The unit is $[\gamma] = m^{-1}.sr^{-1}$.

The total scattering coefficient σ_s is obtained by integrating the volume scattering function $\gamma(\theta)$ over whole solid angle:

$\sigma_s = {}_0\int^{4\pi} \gamma(\theta)\ d\omega,$

or for scattering with rotational symmetry with respect to the incident beam

$\sigma_s = 2\pi._0\int^{\pi} \gamma(\theta)\ \sin(\theta)\ d\theta.$

The scattering coefficient can be understood as the fraction of the light flux scattered per unit length out of a parallel beam of light, its unit is $[\sigma_s] = m^{-1}$. Both the volume scattering function and the scattering coefficient are extensive properties.

The phase function is an intensive property and describes the relative angular dependence of the scattered light of a volume element of particles. For the phase function $P(\theta)$ we have used the following definition: $P(\theta) = 4.\pi.\gamma(\theta)/\sigma_s$.

The angular distribution of the scattered light frequently is characterized by two parameters:

The asymmetry parameter g is obtained by folding the phase function with cos (θ), therefore

$g = \tfrac{1}{2}\ {}_0\int^{\pi} P(\theta)\ \sin(\theta)\ \cos(\theta)\ d\theta.$

The asymmetry parameter is zero for symmetric scattering such as Rayleigh scatter of the air molecules and g=1 for only forward scatter. Another characteristic is the fraction b of the back scattered radiation. It is obtained by integrating

$\tfrac{1}{2}\ P(\theta)\ \sin(\theta)$ between $\tfrac{1}{2}\pi$ and π. Both parameters g and b are intensive.

The lidar ratio, S, is defined as the ratio of the extinction coefficient, σ_e and the volume scattering function at 180°, $\gamma(180°)$, i.e. $S = \sigma_e / \gamma(180°)$, or $S = 4\pi / ([P(180°)\ .\omega]$, with ω the single scattering albedo, i.e. the ratio of the scattering coefficient to the extinction coefficient. The single scattering albedo cannot be measured directly with the polar nephelometer. We have

Formatiert: Schriftart: (Standard) +Textkörper (Times New Roman)

Formatiert: Schriftart: (Standard) +Textkörper (Times New Roman)

used values for ω, which were obtained by inverting data from sun and sky photometers during this study. The average for the Sahara aerosol was ω =0.928 and ω= 0.943 for the non-Sahara aerosol. These values are in agreement with previous findings (Valenzuela et. al. 2012a,b)

The measurement of the scattering coefficient at three wavelengths (e.g. with an integrating nephelometer, Charlson et al., 1967) permitted the determination of the wavelength dependence of the scattering coefficient. In many cases it can be represented by a power law relation $\sigma(\lambda) = \sigma(\lambda_0)\cdot(\lambda/\lambda_0)^{\alpha}$ with α the Ångström exponent (Ångström 1929, 1930). The value of α is independent of the absolute magnitude of the scattering coefficient, i.e. the concentration of the particles. But it is different for different types of aerosols and mainly influenced by the size distribution of the particles. For a power law number size distribution given by $dn/dr = n_0.(r/r_0)^{-\nu}$, the exponent α can be obtained by $\alpha = 3 - \nu$. (Junge 1963). For an aerosol with a size distribution having $\nu > 3$, the smaller particles dominate and $\alpha < 0$~~-1~~, i.e. the scattering coefficient decreases with increasing wavelength. This is the normal case. If the particles are larger than a few micrometers, then $\nu < 3$ and the Ångström exponent is zero or even positive. A strong wavelength dependence of the scattering coefficient ($\alpha < -1$) is an indication for the non-Sahara~~usual~~ aerosol, whereas little or almost no dependence on wavelength is a sign for an ~~desert~~ aerosol containing larger particles, in this study mainly desert particles.

3. Instrument and methods

The volume scattering function of the aerosol has been determined by a custom made polar nephelometer, its design is similar to the one of Waldram (1945), see figure 2: Light from a 532 nm solid state laser of 10 mW power shines into a light trap and illuminates the particles within the beam. A photomultiplier with a collimation optic is mounted on a goniometer and can measure scattered light between 5 and 175°. The scattering volume is approximately 70 mm^3 at 90° scattering angle, increasing to 800 mm^3 at 5° and 175° respectively. Measurements are taken at intervals of 5°, in the near forward direction at 1 to 2°. For one volume scattering function a scan from 175° to 5° and back is made and the average is used. One full scan takes 35 minutes, which can pose a problem with rapidly changing aerosols. Therefore a check for differences between the forward and the back scan is made and if the difference was larger than a factor of 1.5 the data were not used. The instrument is enclosed in an airtight housing; by sucking air out of the enclosure, air from outside can be brought into the instrument. Calibration is done by filling the instrument with carbon dioxide, whose volume scattering function is well known. For all data reported below, the scattering of the air molecules has been subtracted, i.e. all scattering functions, phase functions, asymmetry parameters or back scattered fractions are for aerosol particles only.

Experimentally it is impossible to measure the volume scattering function between 0 to 5°, and 175° to 180°; but the contribution of this range cannot be neglected, especially the forward region. The measured volume scattering function and

its shape between 10° and 5° and 170° and 175° can be used to extrapolate the missing regions. This can be done with an accuracy of better than 5% (Horvath, 2015), thus the complete scattering function is available.

The flow rate through the instrument was 3.3×10^{-4} m^3 s^{-1}. The connection to the sampling inlet of the field laboratory was by a slightly downwards inclined hose of a diameter of 10 mm and a length of 2.5 m. Using data given by given by Hinds (1999, Chapter 10), the loss of particles due to sedimentation in the tube amounted to 10%, 2%, and 0.3% for particles with diameters of 10, 5, and 2 µm. Losses due to diffusion were below 0.02%. Thus it can be concluded, that for the most important particles sizes below 5 µm the sampling losses are negligible.

A TSI 3563 Integrating Nephelometer was used to measure the scattering coefficient for red (700 nm), green (550 nm), and blue (450 nm) light. A detailed description of the instrument and its operation can be found at the NOAA website https://www.esrl.noaa.gov/gmd/aero/instrumentation/neph_desc.html.

Sampling took place in the Albergue Universitario of the University of Granada, located in the Sierra Nevada at an elevation of 2505 m a.s.l. Its coordinates are 37° 5' 43.72"N, 3° 23' 12.57"W. The surrounding mountains had elevations of approx. 3000 m, extending at distances of 20 km from the sampling location. All~~The~~ instruments were located in a room below the flat roof of the building. A pipe with a diameter of 10 cm extended 2.1 m above the roof and into the laboratory. A blower maintained a flow of 0.00167 m^3s^{-1}, all instruments used in the SLOPE campaign (Integrating Nephelometer, Aerodynamic Partice Sizer (APS), Multi Angle Absorption Photometer (MAAP), Scanning Mobility Particle Spectrometer (SMPS), Aethalometer (A33)), and the polar nephelometer) sampled from this pipe. The residence time of the air in the pipe was 0.6 s . Losses in the pipe can be considered negligible.

Measurements were made in the framework of the SLOPE (**S**ierra Nevada **L**idar Aer**O**sol **P**rofiling **E**xperiment) campaign between June 6 and 30, 2016. This campaign mainly was intended to determine the vertical structure of the aerosol by remote sensing instruments and test the various retrieval schemes for obtaining microphysical and optical properties. So the main instruments were sun and sky photometers, multiwavelength lidar, and an airplane. Obviously ground based instruments were also used, as described above.~~,~~ The polar nephelometer could not be operated ~~but not~~ continuously, due to instrument~~s~~ failures and absence of the operator; still, in total 120 phase functions were determined. During this time several intrusions of Sahara dust occurred, usually the dust was layered and could be recognized with the unaided eye.[1] For distinguishing dust aerosols from others, two methods have been applied: (1) The size of the dust particles is larger than

[1] From May to September 2016 there were a total of 15 Sahara dust events, on 96 days out of 153. For details see https://www.mapama.gob.es/es/calidad-y-evaluacion-ambiental/temas/atmosfera-y-calidad-del-aire/episodiosnaturales2016_tcm30-379284.pdf. In June 2016 the events were on the following days: 2-3, 6-11, and 21-30.

Formatiert: Schriftart: Fett
Formatiert: Schriftart: Fett
Formatiert: Schriftart: Fett
Formatiert: Schriftart: Fett
Formatiert: Schriftart: Fett
Formatiert: Englisch (USA)
Formatiert: Englisch (USA)

1µm, thus the Angström exponent normally is larger than -1, whereas the non_Sahara~~usual~~ aerosol has Angström exponents below -1. (2) Using 72 hour back trajectories (from the NOAA HYSPLIT web site, Draxler & Rolph, 2003), the likely origin of the particles can be estimated. Since the Sierra Nevada is a small mountain range, most of the time the air masses reached the measuring location (at an elevation of 2500 m a.s.l.) without admixing or particles of possible nearby sources. The origin of the air mass was classified in a total of six groups. Figure 3 shows the typical situations: Sahara, Sahara high, Atlantic, Atlantic North, Atlantic/Sahara, North Africa/Mediterranean. From the source region in the Sahara to the receptor region in the Sierra Nevada the particles traveled around 1500 km. Table 1 characterizes the 6 types, which occurred during this campaign.

A plot of the Angström exponent as a function of time measured with the three wavelength integrating nephelometer is shown in Figure 4. The classification using the back trajectories is given above. It is evident, that for aerosols influenced by the Sahara, the Angström exponent is larger than -1, thus the two methods of determining Sahara aerosols agree in most of the cases.

4. Results

An overview of the scattering coefficient obtained by integration of the measured volume scattering function and the value measured with the Integrating Nephelometer is shown in figure 5, only the scattering of the particles is plotted, i.e. the Rayleigh scattering of the air was subtracted. The data obtained with the Integrating Nephelometer are values, taken at intervals of minutes, and depict also the variability of the layered aerosol. The scattering coefficient obtained by integration of the polar nephelometer data are averages of about 35 minutes. Agreement between the two datasets is evident. Three periods of measurements can be seen. During Period 1 mostly a distinct intrusion of Sahara Aerosol was observed, except for the beginning, in Period 2 mainly aerosol from the Atlantic reached the site, whereas during Period 3 again Sahara particles dominated the aerosol. The air masses passing over the Atlantic had a much lower scattering coefficient, being about twice the one of pure air.

A plot of all Sahara and non-Sahara Phase functions is depicted in figure 6. There is some scatter in the data due to the layered aerosol, but it is evident, that the phase functions of the Sahara and non-Sahara aerosol are different. The averages of all phase functions of definite Sahara origin and of definite non-Sahara origin are shown in figure 7.

5. Discussion

The comparison between the two types of average phase functions of figure 7 shows definite differences. The non-Sahara (mainly Atlantic) phase function has less forward scatter (on the average 31 sr^{-1} at 0°) than the Sahara phase function (62 sr^{-1}). This is readily explained by the larger size of the desert particles. Whereas spherical particles are a good approximation for the near forward scattering, the smaller backscattering of the Sahara phase function compared to the non-Sahara particles only can be explained by the irregular shape of the particles; For spherical large particles interferences and resonances are most pronounced, which leads to a considerable increase in backscattering and a low side scattering, which both have not been observed. For irregular shaped particles which furthermore are randomly oriented by Brownian rotation, the backscattering is by far less up to a factor of 10 compared to spherical particles, see e.g. Von Hoyningen-Huene and Posse (1997) or Mishchenko et al. (1997), Mishchenko (2000), Nousiainen and Kandler (2015). ~~Another effect of the irregular shape of the Saharan particles is their higher side scattering around 80 to 140°, as has been observed also in this study.~~

The complete volume scattering function or phase function can be used to determine derived properties. The scattering coefficient is obtained by integrating the volume scattering function over the full solid angle. A comparison with the calculated and the measured scattering coefficient was shown in figure 5, the agreement is evident.

For modelling of e.g. radiative transfer, the asymmetry parameter of an aerosol is an important parameter. It is obtained by folding the phase function with the cosine of the scattering angle. For the average phase functions shown in figure 7 the asymmetry parameter for the Sahara aerosol particles is 0.71~~06~~ with a standard deviation of 0.03~~1~~, for the non-Sahara particles it is 0.56~~2~~±0.04~~7~~. The difference is significant, therefore the asymmetry parameter is a good indicator for the desert aerosol. In figure 4~~5~~ the measured asymmetry parameter is added to the graph of the Angström exponent and the origin of the aerosol. Whenever the origin of the aerosol indicates desert particles the asymmetry parameter is high. At the same time the Angström exponent also is high. Figure 8 is a plot of all the data points and shows the relationship between Angström exponent and the asymmetry parameter for all measured phase functions for which Integrating Nephelometer data and polar nephelometer data were available simultaneously. Evidently a larger asymmetry parameter is associated with a larger Angström exponent, but the relationship is not very pronounced.

The scattering function of the desert aerosol has a low back scattering, which is typical for non-spherical particles. Therefore it is to be expected, that a characterization of desert aerosol particles could be achieved by considering the fraction of backscattered light. It is defined as the ratio of integral of the volume scattering function between 90 and 180° divided by the integral over the full angle and is readily available once the volume scattering function is known. A time series of the backscattered fraction obtained in this way is shown in Figure 9, black squares; The back scattered fraction obtained from polar nephelometer measurements is lower for the aerosol dominated by desert particles, as expected; but less distinct than the asymmetry parameter. Furthermore the back scattered fraction obtained with the Integrating Nephelometer (red line) is systematically larger, which has the following reason: The backscattered fraction for the Integrating Nephelometer is obtained by dividing the signals BbsG (signal of the Nephelometer in the backscattering range for green light) by BsG

(signal of the total scattered light). Both signals are proportional to the light flux scattered by the aerosol, but they are truncated, since it is experimentally impossible integrate the scattered light flux from 90° to 180° and 0° to 180° respectively. But the measured volume scattering functions permits the simulation of the truncation effect; and for a range of the scattering angles between 8° and 170° the simulated BbsG is obtained by integrating the measured volume scattering function from 90 to 170° and BsG is obtained by integrating the measured volume scattering function from 8 to 170°. The simulated truncated backscatters fraction is calculated by dividing the simulated Bbsg by the simulated BsG. -The expected signal is also shown (blue circles), which is in much better agreement with the Integrating Nephelometer data.

For the Sahara-particle dominated aerosol the asymmetry parameter is larger and the back scattered fraction is smaller than for the non-Sahara~~usual~~ aerosol. So it is obvious to use both parameters to characterize the Sahara aerosol. A plot of all data points in the (b,g) plane is shown in figure 10. The points representing the Sahara aerosol and the non-Sahara aerosol are well separated. The curve gives the relationship between the backscattered fraction and the asymmetry parameter calculated for monomodal spherical particles. For other refractive indices or ellipsoidal particles an almost identical curve is obtained, the point of inflection is at a slightly different location. For bimodal size distributions the data points are located to the right of the curve (Horvath et al., 2016), as it is the case for the data of this study. A clear distinction between the points representing Sahara and non-Sahara particles is possible. Additionally, points are plotted, which were obtained in Kyoto, Japan, during an event of long range transport dust intrusion from the Gobi Desert. These data perfectly fit together with the Sahara data.

6. Conclusion

The volume scattering function of the atmospheric aerosol was measured in the Sierra Nevada, where intrusions of Sahara aerosol are frequent. The origin of the aerosol particles was determined by back trajectories and/or by the Angström exponent of the wavelength dependence of the scattering coefficient of the aerosol.

The phase function of the Sahara aerosol has more forward scatter, less back scatter and more side scatter; it is more asymmetric than the non-Sahara aerosol, which in this study was mainly marine, with little continental influence. A few parameters of the aerosol are listed in table 2.

The best distinction between Sahara and non-Sahara aerosol is possible when using the asymmetry parameter, as is evident also in figures 5 and 11. This study suggests that particles causing an asymmetry parameter of the phase function above a value of 0.65 could be considered of Sahara desert origin. The asymmetric scattering of the Gobi desert aerosol is very similar to the one of the Sahara Aerosol.

Acknowledgements

This work was supported by the Andalusia Regional Government through project P12-RNM-2409, by the Spanish Agencia Estatal de Investigación, AEI, through projects CGL2016-81092-R and CGL2017-90884-REDT. We acknowledge the financial support by the European Union's Horizon 2020 research and innovation program through project ACTRIS-2 (grant agreement No 654109). The authors thankfully acknowledge the FEDER program for the instrumentation used in this work and the University of Granada that supported this study through the Excellence Unit Program.

~~This work was supported by the Andalusia Regional Government through project P12-RNM-2409, by the Spanish Ministry of Economy and Competitiveness through project CGL2016-81092-R. we acknowledge the financial support by the European Union's Horizon 2020 research and innovation program through project ACTRIS-2 (grant agreement No 654109). The authors thankfully acknowledge the FEDER program for the instrumentation used in this work.~~

References

Alfaro, S. C., Gomez, L., Rajot, J. L., Lafon, S., Gaudichet, A., Chatenet, B., Maille, M. ; Cautenet, G. ; Lasserre, F. ; Cachier, H. ; Zhang, X. Y. (2003). Chemical and optical characterization of aerosols measured in spring 2002 at the ACE-Asia supersite Zhenbeitai China. Journal of Geophysical Research, 108(D23), 8641.

Ångström A. (1929) On the atmospheric transmission of sun radiation and on dust in the atmosphere. Geogr. Annaler, Stockholm, 11,156-166

Ångström A. (1930) On the atmospheric transmission of sun radiation II. Geogr. Annaler, Stockholm, 12, 130-159

Antón M, A. Valenzuela, D. Mateos, I. Alados , I. Foyo-Moreno, F.J. Olmo, L. Alados-Arboledas (2014) Longwave aerosol radiative effects during an extreme desert dust event in southeastern Spain. Atmospheric Research, 148, 18–23

Charlson R.J., H. Horvath, R.F. Pueschel (1967) The direct measurement of atmospheric light scattering coefficient for studies of visibility and pollution Atm. Environment 1, pp. 469-478, 1967

Cheng, T., Lu, D., Chen, H., & Xu, Y. (2005). Physical characteristic of dust aerosol over Husan Dake sandland in Northern China. Atmospheric Environment, 39, 1237–1243.

Draxler, R. R., & Rolph, G. D. (2003). HYSPLIT (HYbrid Single-Particle Lagrangian Integrated Trajectory) Model access via NOAAARL READY Website (http://www.arl.noaa.gov/ready/hysplit4.html). NOAA Air Resources Laboratory, Silver Spring, MD.

Falkovich, A. H., Gomez, E., Lewin, Z., Formenti, P., & Rudich,Y. (2001). Analysis of individual dust particles. Journal of Geophysical Research, 29 106(D16), 18029–18036.

Hinds, W. C. (1999). Aerosol technology: Properties, behavior, and measurement of airborne particles (2nd ed.). NewYork, NY, 483pp.

H. Horvath (2015), Extrapolation of a truncated aerosol volume scattering function to the far forward and back region, Journal of Aerosol Science, http://dx.doi.org/10.1016/j.jaerosci.2015.08.001

H. Horvath, M. Kasahara, S. Tohno, F. J. Olmo, H. Lyamani, L. Alados-Arboledas, A. Quirantes, V. Cachorro (2016) Relationship between fraction of backscattered light and asymmetry parameter Journal of Aerosol Science 91, 43-53, 2016 DOI: 10.1016/j.jaerosci.2015.09.003

IPCC (2001) Climate Change 2001 - IPCC Third Assessment Report, the scientifc basis,chapter_5.2.2.1 Soil dust, Table 5.3 (available at https://www.ipcc.ch/ipccreports/tar/wg1/168.htm)

Iwasaka,Y., Shi, G.-Y.,Yamada, M., Matsuki, A., Trochkine, D., Kim,Y. S. et al. (2003). Importance of dust particles in the free troposphere over theTaklaman desert: Electron microscopic experiments of particles collected with a baloonborne particle impactor at Dunhunag, China. Journal of Geophysical Research, 108(D23), 8644.

Jaenicke, R. (1988). Aerosol Physics and Chemistry in Zahlenwerte und Funktionen aus Naturwissenschaft und Technik, Landolt Börnstein, Group 5 (Vol. 4, subvolume b), Physikalische und chemische Eigenschaften der Luft. Berlin, Germany: Springer.

Junge Ch. (1979) The importance of mineral dust as an atmospheric constituent. Chapter 2 of *Saharan Dust; mobilization, transport, deposition*. C. Morales, Ed.; John Wiley & Sons, pp. 49 - 60

Kandler K., Benker N., Bundke U.,Cuevas E., Ebert M.,, Knippertz E., Rodriguez S.,Schütz L., Weinbruch S., (2007) Chemical composition and complex refractive index of Saharan Mineral Dust at Izana, Tenerife (Spain) derived by electron microscopy. Atmospheric Environment 41 8058–8074

Kontratyev, K. Ya., Ivlev, L. S., Krapivin, V. F., & Varostos, C. A. (2006). Atmospheric aerosol properties. Formation, processes, impacts. Berlin: Springer, p. 141.

Mishchenko M.I., Hovenier J.W., Travis L.D. , Eds. (2000) Light scattering by nonsperical particles, theory, measurements and applications. Academic Press, 690 pp

Mishchenko, M. I., Travis, L. D., Kahn, R. A., & West, R. A. (1997). Modeling phase functions for dustlike tropospheric aerosols using a shape mixture of randomly oriented polydisperse spheroids. Journal of Geophysical Research, 102, 16831–16847.

Nousiainen T. and Kandler K. (2015) Light scattering by atmospheric mineral dust particles. In Light Scattering Reviews 9: Light Scattering and Radiative Transfer. A. Kokhanovsky, Ed. pp 3-52 Springer Praxis Books

Obregón M.A., Pereira S., Salgueiro V., Costa M.J,. Silva A.M, Serrano A., Bortoli D. Aerosol radiative effects during two desert dust events in August 2012 over the Southwestern Iberian Peninsula. Atmospheric Research, 2015; 153: 404 DOI: 10.1016/j.atmosres.2014.10.007

Von Hoyningen-Huene,W., & Posse, P. (1997). Nonsphericity of aerosol particles and their contribution to radiative forcing. Journal of Quantative Spectroscopy & Radiative Transfer, 57, 651–668.

Formatiert: Schriftart: Nicht Fett, Englisch (USA)

Formatiert: Schriftart: Nicht Fett

Formatiert: Schriftart: Nicht Fett, Englisch (USA)

Formatiert: Schriftart: Nicht Fett

Formatiert: Englisch (USA)

Formatiert: Englisch (USA)

Formatiert: Englisch (USA)

Formatiert: Englisch (USA)

Formatiert: Englisch (USA)

Formatiert: Englisch (USA)

Formatiert: Englisch (USA)

Valenzuela A., F. J. Olmo, H. Lyamani, M. Antón, A. Quirantes, and L. Alados-Arboledas (2012a) Aerosol radiative forcing during African desert dust events (2005–2010) over Southeastern Spain. Atmos. Chem. Phys., 12, 10331–10351

Valenzuela A., F. J. Olmo, H. Lyamani, M. Antón, A. Quirantes, and L. Alados-Arboledas (2012b) Classification of aerosol radiative properties during African desert dust intrusions over southeastern Spain by sector origins and cluster analysis. Journal of Geophysical Research 117 D06214 doi:10.1029/2011JD016885, 2012

Waldram, J. M. (1945). Measurement of the photometric properties of the upper atmosphere. Trans. Illum. Eng. Soc., 10, 147–188.

Xin, J.,Wang, S.,Wang,Y.,Yuan, J., Zhang,W., & Sun,Y. (2005). Optical properties and size distribution of dust aerosols over the Tengger Desert in Northern China. Atmospheric Environment, 39, 5971–5978.

Formatiert: Englisch (USA)

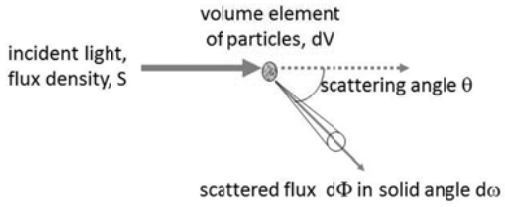

Figure 1: Definition of volume scattering function

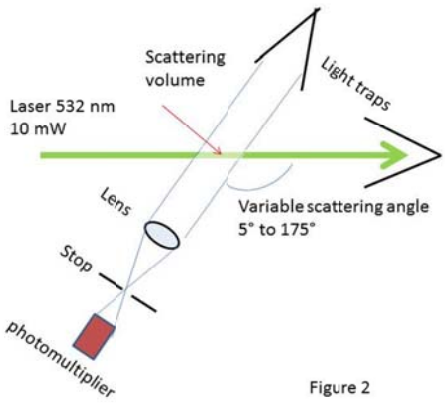

Figure 2: Principle of the polar nephelometer

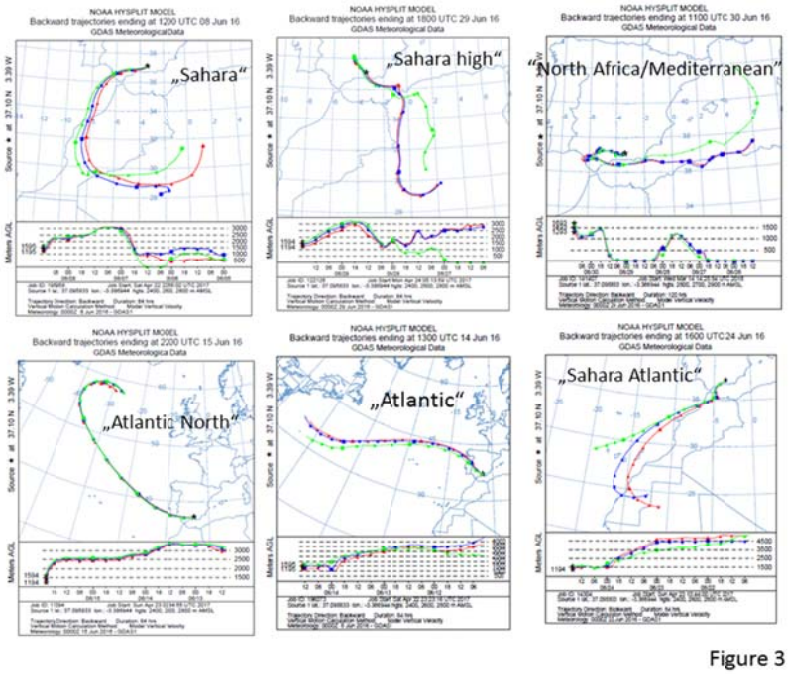

Figure 3: Back trajectories used for classification of aerosol types

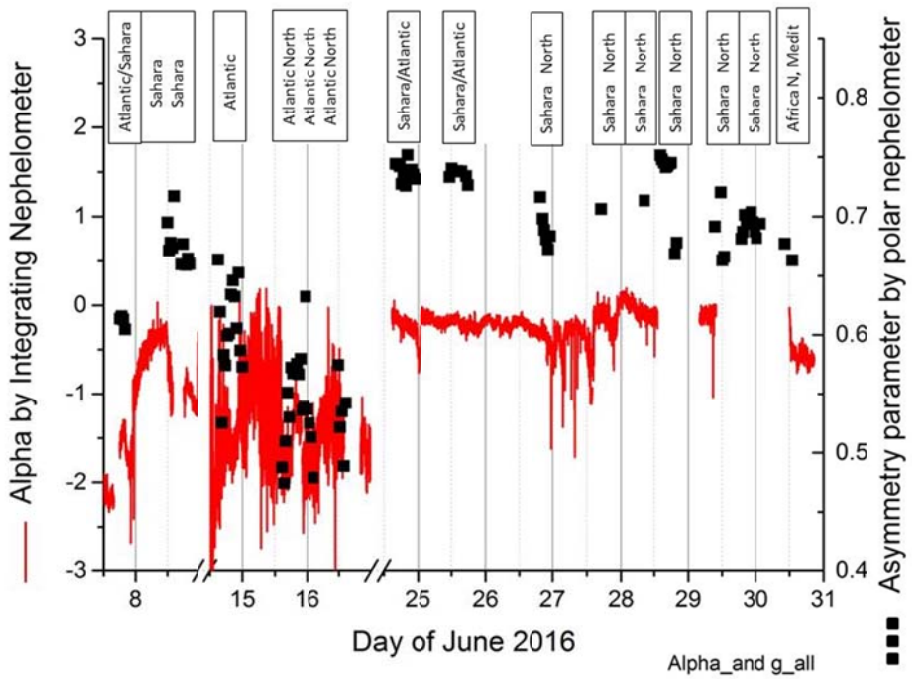

Figure 4: Angström exponent of the spectral scattering coefficient of the aerosol measured and classification by back trajectories. For the desert aerosol the Angström Exponent is larger than -1. In addition the asymmetry parameter is plotted too, for desert aerosol it is larger than 0.65.

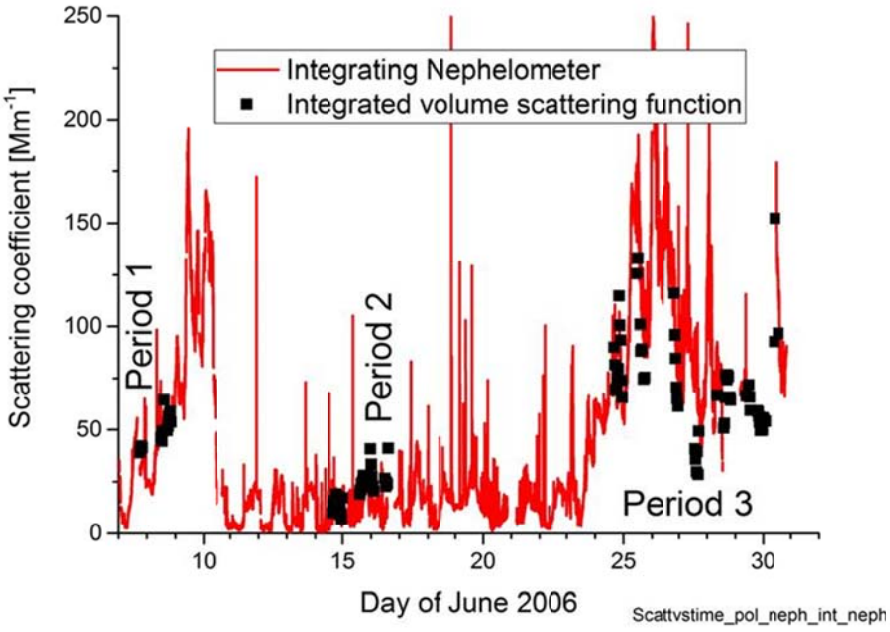

Figure 5: Measured scattering coefficient of the aerosol during the three periods of observation. The solid red line is the signal of the Integrating Nephelometer, the points are scattering coefficients obtained by integrating the measured volume scattering function.

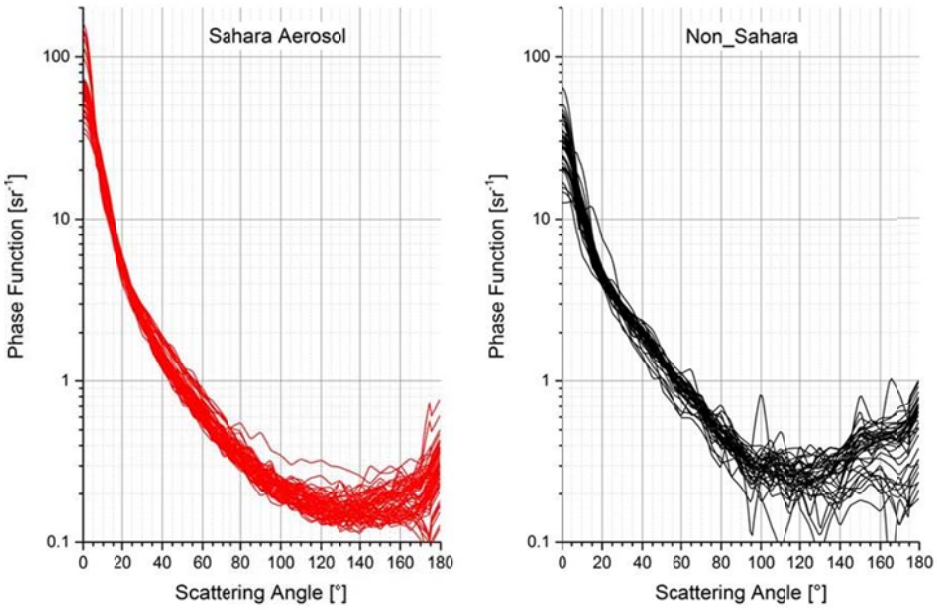

Figure 6. Comparison of phase function attributed to Sahara and non-Sahara aerosols.

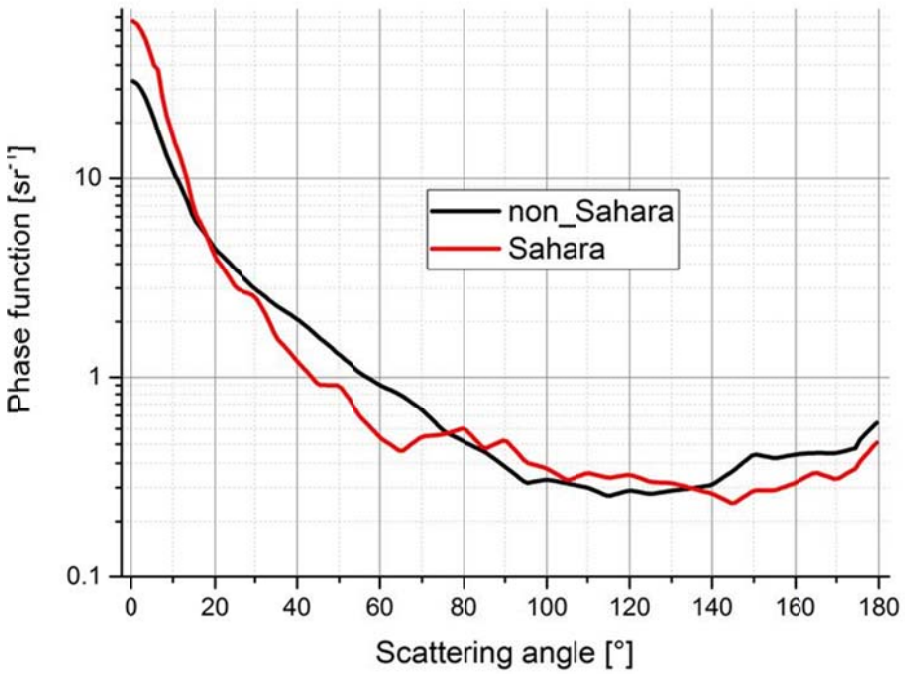
Phase function [sr⁻¹]
10
1
0.1
0
20
40
60
80
100
120
140
160
180
Scattering angle [°]
non_Sahara
Sahara

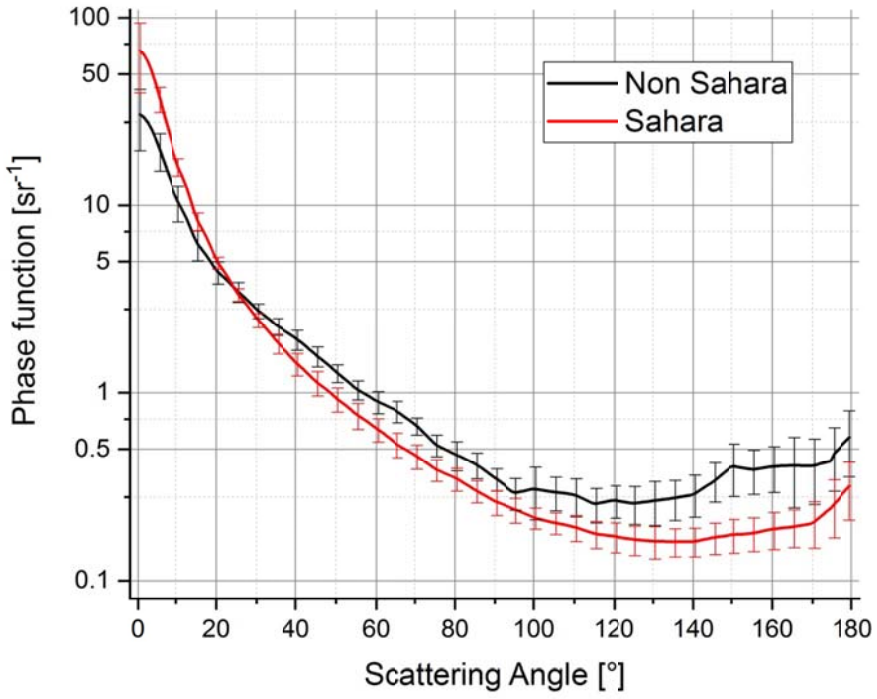

~~Figure~~ Figure 7. Average of the Sahara and non-Sahara aerosol phase functions.

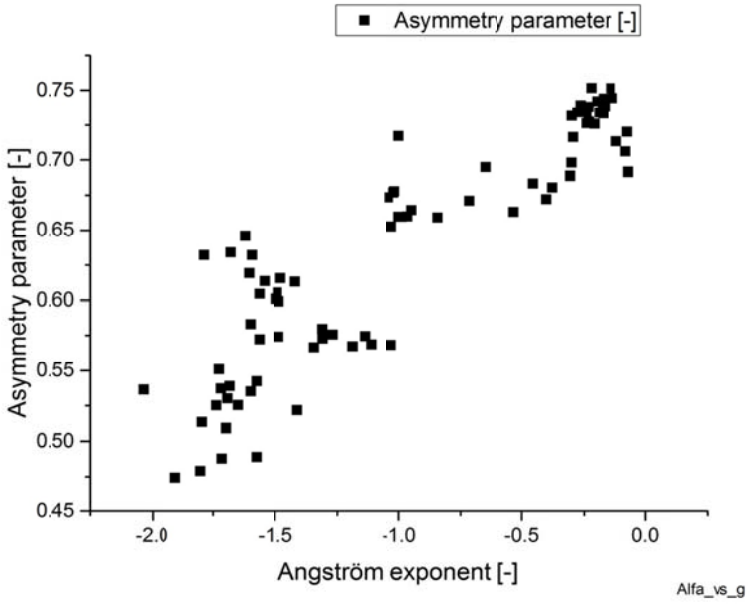

Figure 8. Relationship between the measured Angström exponent and the asymmetry parameter using the measured phase function.

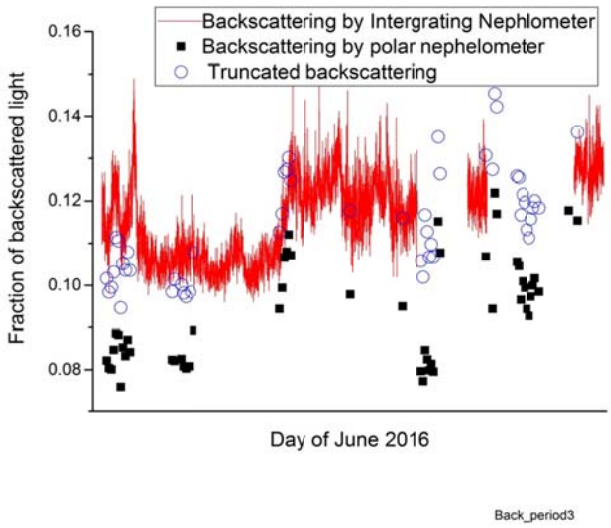

Figure 9. Back scattered fraction measured with the Integrating Nephelometer (red curve) and values obtained by the measured Volume scatteing function. Simulation of the truncation is shown by the hollow points.

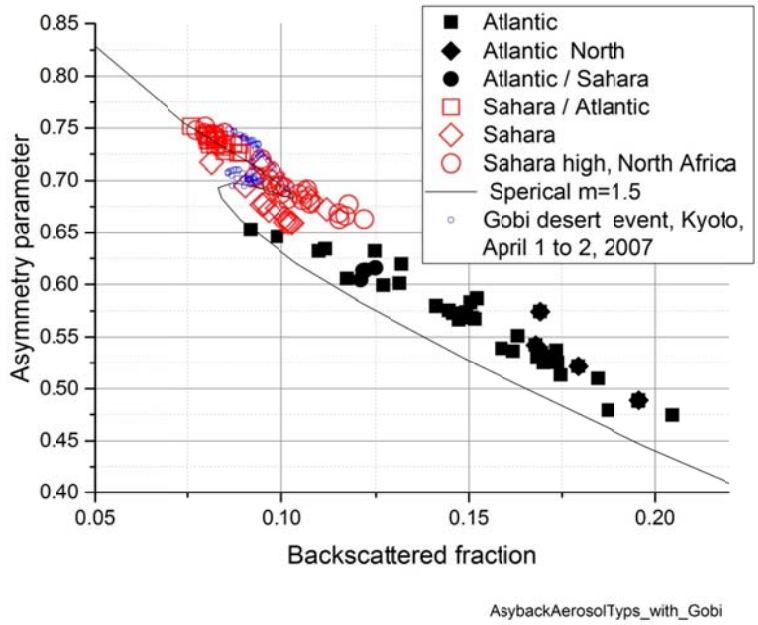

Figure 10: Asymmetry parameter and backscattered fraction calculated for the aerosols measured during this study. A clear separation between Sahara and non-Sahara aerosols is evident. The data points are in excellent agreement with data for the Gobi Desert aerosol.

Table 1. Classification of back trajectories		
Name	Air passes over	Remark
„Atlantic“	60°W<longitude<0°, 35°N<latitude<40°N	
“Atlantic North”	40°W<longitude<0°, 60°N<latitude<40°N	
“Sahara”	10°W<longitude<5°E,37°N<latitude<26°N	
“Sahara high”	5°W<longitude<5°E, 37°N<latitude<26°N	
“Sahara/Atlantic”, “Atlantic/Sahara” resp.	Up to 500 km West of the coast of Africa	Distinction between the two by Angström exponent
“North Africa/Mediterranean”	6°W<longitude<8°E, 35°N<latitude<37°	

5

Table 2. Characteristics of the two types of aerosols				
	Sahara aerosol		Non-Sahara Aerosol	
	Value	Stddev.	Value	Stddev.
Asymmetry parameter [-]	0.7106	0.032	0.562	0.0547
Backscattered fraction [-]	0.094	0.014	0.153	0.027
Average scattering coefficient [Mm^{-1}]	71	22	22.3	7.3
Phase function at 0° [sr^{-1}]	67	27	31	10
Phase function at 90° [sr^{-1}]	0.26	0.034	0.35	0.04
Phase function at 180° [sr^{-1}]	0.31	0.11	0.59	0.21
Lidar ratio [sr^{-1}]	44	16	23	8

The mechanical production of particles results in particle sizes usually larger than 1 µm. Mean sizes range up to 10µm (Kontratyev et al. (2006), Alfaro et al. (2003), Cheng et al. (2005), Xin et al. (2005), Alfaro & Gomez, (2001), Falkovich et al., (2001)), and during atmospheric transport the size distribution is modified, mainly due to the shorter life time ~~settling of~~ of larger particles: The average residence time in the troposphere is estimated as 10 days for 1 µm particles and 3 days for 10 µm particles. (Jaenicke, 1988)

Since the dust particles have an irregular shape, their scattering properties are difficult to model, but their scattering properties are urgently needed to estimate the effect on climate. Below we report measurements of the volume scattering function of the Sahara aerosol transported to the Iberian Peninsula, which were performed during several dust outbreaks.

2 Definitions, units, and nomenclature

The volume scattering function $\gamma(\theta)$ of the aerosol is defined as follows, see figure 1: Let a volume dV of aerosol be illuminated by radiation having a flux density S. The light flux $d\Phi$ scattered into a solid angle $d\omega$ at the scattering angle θ is obtained as

$d\Phi = E\ S.\ \gamma(\theta)\ .\ d\omega\ .\ dV.$ The unit is $[\gamma] = m^{-1}.sr^{-1}$.

The total scattering coefficient σ_s is obtained by integrating the volume scattering function $\gamma(\theta)$ over whole solid angle:

$\sigma_s = {}_0\int^{4\pi} \gamma(\theta)\ d\omega,$

or for scattering with rotational symmetry with respect to the incident beam

$\sigma_s = 2\pi._0\int^{\pi} \gamma(\theta)\ \sin(\theta)\ d\theta.$

The scattering coefficient can be understood as the fraction of the light flux scattered per unit length out of a parallel beam of light, its unit is $[\sigma_s] = m^{-1}$. Both the volume scattering function and the scattering coefficient are extensive properties.

The phase function is an intensive property and describes the relative angular dependence of the scattered light of a volume element of particles. For the phase function $P(\theta)$ we have used the following definition: $P(\theta) = 4.\pi.\gamma(\theta)/\sigma_s$.

The angular distribution of the scattered light frequently is characterized by two parameters:

The asymmetry parameter g is obtained by folding the phase function with cos (θ), therefore

$g = \tfrac{1}{2}\ {}_0\int^{\pi} P(\theta)\ \sin(\theta)\ \cos(\theta)\ d\theta.$

The asymmetry parameter is zero for symmetric scattering such as Rayleigh scatter of the air molecules and g=1 for only forward scatter. Another characteristic is the fraction b of the back scattered radiation. It is obtained by integrating

$\tfrac{1}{2}\ P(\theta)\ \sin(\theta)$ between $\tfrac{1}{2}\pi$ and π. Both parameters g and b are intensive.

The lidar ratio, S, is defined as the ratio of the extinction coefficient, σ_e and the volume scattering function at 180°, $\gamma(180°)$, i.e. $S = \sigma_e / \gamma(180°)$, or $S = 4\pi / ([P(180°)\ .\omega]$, with ω the single scattering albedo, i.e. the ratio of the scattering coefficient to the extinction coefficient. The single scattering albedo cannot be measured directly with the polar nephelometer. We have

Formatiert: Schriftart: (Standard) +Textkörper (Times New Roman)

Formatiert: Schriftart: (Standard) +Textkörper (Times New Roman)

used values for ω, which were obtained by inverting data from sun and sky photometers during this study. The average for the Sahara aerosol was ω =0.928 and ω= 0.943 for the non-Sahara aerosol. These values are in agreement with previous findings (Valenzuela et. al. 2012a,b)

The measurement of the scattering coefficient at three wavelengths (e.g. with an integrating nephelometer, Charlson et al., 1967) permitted the determination of the wavelength dependence of the scattering coefficient. In many cases it can be represented by a power law relation $\sigma(\lambda) = \sigma(\lambda_0)\cdot(\lambda/\lambda_0)^{\alpha}$ with α the Ångström exponent (Ångström 1929, 1930). The value of α is independent of the absolute magnitude of the scattering coefficient, i.e. the concentration of the particles. But it is different for different types of aerosols and mainly influenced by the size distribution of the particles. For a power law number size distribution given by $dn/dr = n_0.(r/r_0)^{-\nu}$, the exponent α can be obtained by $\alpha = 3 - \nu$. (Junge 1963). For an aerosol with a size distribution having $\nu > 3$, the smaller particles dominate and $\alpha < 0$~~-1~~, i.e. the scattering coefficient decreases with increasing wavelength. This is the normal case. If the particles are larger than a few micrometers, then $\nu < 3$ and the Ångström exponent is zero or even positive. A strong wavelength dependence of the scattering coefficient ($\alpha < -1$) is an indication for the non-Sahara~~usual~~ aerosol, whereas little or almost no dependence on wavelength is a sign for an ~~desert~~ aerosol containing larger particles, in this study mainly desert particles.

3. Instrument and methods

The volume scattering function of the aerosol has been determined by a custom made polar nephelometer, its design is similar to the one of Waldram (1945), see figure 2: Light from a 532 nm solid state laser of 10 mW power shines into a light trap and illuminates the particles within the beam. A photomultiplier with a collimation optic is mounted on a goniometer and can measure scattered light between 5 and 175°. The scattering volume is approximately 70 mm^3 at 90° scattering angle, increasing to 800 mm^3 at 5° and 175° respectively. Measurements are taken at intervals of 5°, in the near forward direction at 1 to 2°. For one volume scattering function a scan from 175° to 5° and back is made and the average is used. One full scan takes 35 minutes, which can pose a problem with rapidly changing aerosols. Therefore a check for differences between the forward and the back scan is made and if the difference was larger than a factor of 1.5 the data were not used. The instrument is enclosed in an airtight housing; by sucking air out of the enclosure, air from outside can be brought into the instrument. Calibration is done by filling the instrument with carbon dioxide, whose volume scattering function is well known. For all data reported below, the scattering of the air molecules has been subtracted, i.e. all scattering functions, phase functions, asymmetry parameters or back scattered fractions are for aerosol particles only.

Experimentally it is impossible to measure the volume scattering function between 0 to 5°, and 175° to 180°; but the contribution of this range cannot be neglected, especially the forward region. The measured volume scattering function and

its shape between 10° and 5° and 170° and 175° can be used to extrapolate the missing regions. This can be done with an accuracy of better than 5% (Horvath, 2015), thus the complete scattering function is available.

The flow rate through the instrument was 3.3×10^{-4} m^3 s^{-1}. The connection to the sampling inlet of the field laboratory was by a slightly downwards inclined hose of a diameter of 10 mm and a length of 2.5 m. Using data given by given by Hinds (1999, Chapter 10), the loss of particles due to sedimentation in the tube amounted to 10%, 2%, and 0.3% for particles with diameters of 10, 5, and 2 µm. Losses due to diffusion were below 0.02%. Thus it can be concluded, that for the most important particles sizes below 5 µm the sampling losses are negligible.

A TSI 3563 Integrating Nephelometer was used to measure the scattering coefficient for red (700 nm), green (550 nm), and blue (450 nm) light. A detailed description of the instrument and its operation can be found at the NOAA website https://www.esrl.noaa.gov/gmd/aero/instrumentation/neph_desc.html.

Sampling took place in the Albergue Universitario of the University of Granada, located in the Sierra Nevada at an elevation of 2505 m a.s.l. Its coordinates are 37° 5' 43.72"N, 3° 23' 12.57"W. The surrounding mountains had elevations of approx. 3000 m, extending at distances of 20 km from the sampling location. All~~The~~ instruments were located in a room below the flat roof of the building. A pipe with a diameter of 10 cm extended 2.1 m above the roof and into the laboratory. A blower maintained a flow of 0.00167 m^3s^{-1}, all instruments used in the SLOPE campaign (Integrating Nephelometer, Aerodynamic Partice Sizer (APS), Multi Angle Absorption Photometer (MAAP), Scanning Mobility Particle Spectrometer (SMPS), Aethalometer (A33)), and the polar nephelometer) sampled from this pipe. The residence time of the air in the pipe was 0.6 s . Losses in the pipe can be considered negligible.

Measurements were made in the framework of the SLOPE (**S**ierra Nevada **L**idar Aer**O**sol **P**rofiling **E**xperiment) campaign between June 6 and 30, 2016. This campaign mainly was intended to determine the vertical structure of the aerosol by remote sensing instruments and test the various retrieval schemes for obtaining microphysical and optical properties. So the main instruments were sun and sky photometers, multiwavelength lidar, and an airplane. Obviously ground based instruments were also used, as described above.~~,~~ The polar nephelometer could not be operated ~~but not~~ continuously, due to instrument~~s~~ failures and absence of the operator; still, in total 120 phase functions were determined. During this time several intrusions of Sahara dust occurred, usually the dust was layered and could be recognized with the unaided eye.[1] For distinguishing dust aerosols from others, two methods have been applied: (1) The size of the dust particles is larger than

[1] From May to September 2016 there were a total of 15 Sahara dust events, on 96 days out of 153. For details see https://www.mapama.gob.es/es/calidad-y-evaluacion-ambiental/temas/atmosfera-y-calidad-del-aire/episodiosnaturales2016_tcm30-379284.pdf. In June 2016 the events were on the following days: 2-3, 6-11, and 21-30.

Formatiert: Schriftart: Fett
Formatiert: Schriftart: Fett
Formatiert: Schriftart: Fett
Formatiert: Schriftart: Fett
Formatiert: Schriftart: Fett
Formatiert: Englisch (USA)
Formatiert: Englisch (USA)

1µm, thus the Angström exponent normally is larger than -1, whereas the non_Sahara~~usual~~ aerosol has Angström exponents below -1. (2) Using 72 hour back trajectories (from the NOAA HYSPLIT web site, Draxler & Rolph, 2003), the likely origin of the particles can be estimated. Since the Sierra Nevada is a small mountain range, most of the time the air masses reached the measuring location (at an elevation of 2500 m a.s.l.) without admixing or particles of possible nearby sources. The origin of the air mass was classified in a total of six groups. Figure 3 shows the typical situations: Sahara, Sahara high, Atlantic, Atlantic North, Atlantic/Sahara, North Africa/Mediterranean. From the source region in the Sahara to the receptor region in the Sierra Nevada the particles traveled around 1500 km. Table 1 characterizes the 6 types, which occurred during this campaign.

A plot of the Angström exponent as a function of time measured with the three wavelength integrating nephelometer is shown in Figure 4. The classification using the back trajectories is given above. It is evident, that for aerosols influenced by the Sahara, the Angström exponent is larger than -1, thus the two methods of determining Sahara aerosols agree in most of the cases.

4. Results

An overview of the scattering coefficient obtained by integration of the measured volume scattering function and the value measured with the Integrating Nephelometer is shown in figure 5, only the scattering of the particles is plotted, i.e. the Rayleigh scattering of the air was subtracted. The data obtained with the Integrating Nephelometer are values, taken at intervals of minutes, and depict also the variability of the layered aerosol. The scattering coefficient obtained by integration of the polar nephelometer data are averages of about 35 minutes. Agreement between the two datasets is evident. Three periods of measurements can be seen. During Period 1 mostly a distinct intrusion of Sahara Aerosol was observed, except for the beginning, in Period 2 mainly aerosol from the Atlantic reached the site, whereas during Period 3 again Sahara particles dominated the aerosol. The air masses passing over the Atlantic had a much lower scattering coefficient, being about twice the one of pure air.

A plot of all Sahara and non-Sahara Phase functions is depicted in figure 6. There is some scatter in the data due to the layered aerosol, but it is evident, that the phase functions of the Sahara and non-Sahara aerosol are different. The averages of all phase functions of definite Sahara origin and of definite non-Sahara origin are shown in figure 7.

5. Discussion

The comparison between the two types of average phase functions of figure 7 shows definite differences. The non-Sahara (mainly Atlantic) phase function has less forward scatter (on the average 31 sr^{-1} at 0°) than the Sahara phase function (62 sr^{-1}). This is readily explained by the larger size of the desert particles. Whereas spherical particles are a good approximation for the near forward scattering, the smaller backscattering of the Sahara phase function compared to the non-Sahara particles only can be explained by the irregular shape of the particles; For spherical large particles interferences and resonances are most pronounced, which leads to a considerable increase in backscattering and a low side scattering, which both have not been observed. For irregular shaped particles which furthermore are randomly oriented by Brownian rotation, the backscattering is by far less up to a factor of 10 compared to spherical particles, see e.g. Von Hoyningen-Huene and Posse (1997) or Mishchenko et al. (1997), Mishchenko (2000), Nousiainen and Kandler (2015). ~~Another effect of the irregular shape of the Saharan particles is their higher side scattering around 80 to 140°, as has been observed also in this study.~~

The complete volume scattering function or phase function can be used to determine derived properties. The scattering coefficient is obtained by integrating the volume scattering function over the full solid angle. A comparison with the calculated and the measured scattering coefficient was shown in figure 5, the agreement is evident.

For modelling of e.g. radiative transfer, the asymmetry parameter of an aerosol is an important parameter. It is obtained by folding the phase function with the cosine of the scattering angle. For the average phase functions shown in figure 7 the asymmetry parameter for the Sahara aerosol particles is 0.71~~06~~ with a standard deviation of 0.03~~1~~, for the non-Sahara particles it is 0.56~~2~~±0.04~~7~~. The difference is significant, therefore the asymmetry parameter is a good indicator for the desert aerosol. In figure 4~~5~~ the measured asymmetry parameter is added to the graph of the Angström exponent and the origin of the aerosol. Whenever the origin of the aerosol indicates desert particles the asymmetry parameter is high. At the same time the Angström exponent also is high. Figure 8 is a plot of all the data points and shows the relationship between Angström exponent and the asymmetry parameter for all measured phase functions for which Integrating Nephelometer data and polar nephelometer data were available simultaneously. Evidently a larger asymmetry parameter is associated with a larger Angström exponent, but the relationship is not very pronounced.

The scattering function of the desert aerosol has a low back scattering, which is typical for non-spherical particles. Therefore it is to be expected, that a characterization of desert aerosol particles could be achieved by considering the fraction of backscattered light. It is defined as the ratio of integral of the volume scattering function between 90 and 180° divided by the integral over the full angle and is readily available once the volume scattering function is known. A time series of the backscattered fraction obtained in this way is shown in Figure 9, black squares; The back scattered fraction obtained from polar nephelometer measurements is lower for the aerosol dominated by desert particles, as expected; but less distinct than the asymmetry parameter. Furthermore the back scattered fraction obtained with the Integrating Nephelometer (red line) is systematically larger, which has the following reason: The backscattered fraction for the Integrating Nephelometer is obtained by dividing the signals BbsG (signal of the Nephelometer in the backscattering range for green light) by BsG

(signal of the total scattered light). Both signals are proportional to the light flux scattered by the aerosol, but they are truncated, since it is experimentally impossible integrate the scattered light flux from 90° to 180° and 0° to 180° respectively. But the measured volume scattering functions permits the simulation of the truncation effect; and for a range of the scattering angles between 8° and 170° the simulated BbsG is obtained by integrating the measured volume scattering function from 90 to 170° and BsG is obtained by integrating the measured volume scattering function from 8 to 170°. The simulated truncated backscatters fraction is calculated by dividing the simulated Bbsg by the simulated BsG. -The expected signal is also shown (blue circles), which is in much better agreement with the Integrating Nephelometer data.

For the Sahara-particle dominated aerosol the asymmetry parameter is larger and the back scattered fraction is smaller than for the non-Sahara~~usual~~ aerosol. So it is obvious to use both parameters to characterize the Sahara aerosol. A plot of all data points in the (b,g) plane is shown in figure 10. The points representing the Sahara aerosol and the non-Sahara aerosol are well separated. The curve gives the relationship between the backscattered fraction and the asymmetry parameter calculated for monomodal spherical particles. For other refractive indices or ellipsoidal particles an almost identical curve is obtained, the point of inflection is at a slightly different location. For bimodal size distributions the data points are located to the right of the curve (Horvath et al., 2016), as it is the case for the data of this study. A clear distinction between the points representing Sahara and non-Sahara particles is possible. Additionally, points are plotted, which were obtained in Kyoto, Japan, during an event of long range transport dust intrusion from the Gobi Desert. These data perfectly fit together with the Sahara data.

6. Conclusion

The volume scattering function of the atmospheric aerosol was measured in the Sierra Nevada, where intrusions of Sahara aerosol are frequent. The origin of the aerosol particles was determined by back trajectories and/or by the Angström exponent of the wavelength dependence of the scattering coefficient of the aerosol.

The phase function of the Sahara aerosol has more forward scatter, less back scatter and more side scatter; it is more asymmetric than the non-Sahara aerosol, which in this study was mainly marine, with little continental influence. A few parameters of the aerosol are listed in table 2.

The best distinction between Sahara and non-Sahara aerosol is possible when using the asymmetry parameter, as is evident also in figures 5 and 11. This study suggests that particles causing an asymmetry parameter of the phase function above a value of 0.65 could be considered of Sahara desert origin. The asymmetric scattering of the Gobi desert aerosol is very similar to the one of the Sahara Aerosol.

Acknowledgements

This work was supported by the Andalusia Regional Government through project P12-RNM-2409, by the Spanish Agencia Estatal de Investigación, AEI, through projects CGL2016-81092-R and CGL2017-90884-REDT. We acknowledge the financial support by the European Union's Horizon 2020 research and innovation program through project ACTRIS-2 (grant agreement No 654109). The authors thankfully acknowledge the FEDER program for the instrumentation used in this work and the University of Granada that supported this study through the Excellence Unit Program.

~~This work was supported by the Andalusia Regional Government through project P12-RNM-2409, by the Spanish Ministry of Economy and Competitiveness through project CGL2016-81092-R. we acknowledge the financial support by the European Union's Horizon 2020 research and innovation program through project ACTRIS-2 (grant agreement No 654109). The authors thankfully acknowledge the FEDER program for the instrumentation used in this work.~~

References

Alfaro, S. C., Gomez, L., Rajot, J. L., Lafon, S., Gaudichet, A., Chatenet, B., Maille, M. ; Cautenet, G. ; Lasserre, F. ; Cachier, H. ; Zhang, X. Y. (2003). Chemical and optical characterization of aerosols measured in spring 2002 at the ACE-Asia supersite Zhenbeitai China. Journal of Geophysical Research, 108(D23), 8641.

Ångström A. (1929) On the atmospheric transmission of sun radiation and on dust in the atmosphere. Geogr. Annaler, Stockholm, 11,156-166

Ångström A. (1930) On the atmospheric transmission of sun radiation II. Geogr. Annaler, Stockholm, 12, 130-159

Antón M, A. Valenzuela, D. Mateos, I. Alados , I. Foyo-Moreno, F.J. Olmo, L. Alados-Arboledas (2014) Longwave aerosol radiative effects during an extreme desert dust event in southeastern Spain. Atmospheric Research, 148, 18–23

Charlson R.J., H. Horvath, R.F. Pueschel (1967) The direct measurement of atmospheric light scattering coefficient for studies of visibility and pollution Atm. Environment 1, pp. 469-478, 1967

Cheng, T., Lu, D., Chen, H., & Xu, Y. (2005). Physical characteristic of dust aerosol over Husan Dake sandland in Northern China. Atmospheric Environment, 39, 1237–1243.

Draxler, R. R., & Rolph, G. D. (2003). HYSPLIT (HYbrid Single-Particle Lagrangian Integrated Trajectory) Model access via NOAAARL READY Website (http://www.arl.noaa.gov/ready/hysplit4.html). NOAA Air Resources Laboratory, Silver Spring, MD.

Falkovich, A. H., Gomez, E., Lewin, Z., Formenti, P., & Rudich,Y. (2001). Analysis of individual dust particles. Journal of Geophysical Research, 29 106(D16), 18029–18036.

Hinds, W. C. (1999). Aerosol technology: Properties, behavior, and measurement of airborne particles (2nd ed.). NewYork, NY, 483pp.

H. Horvath (2015), Extrapolation of a truncated aerosol volume scattering function to the far forward and back region, Journal of Aerosol Science, http://dx.doi.org/10.1016/j.jaerosci.2015.08.001

H. Horvath, M. Kasahara, S. Tohno, F. J. Olmo, H. Lyamani, L. Alados-Arboledas, A. Quirantes, V. Cachorro (2016) Relationship between fraction of backscattered light and asymmetry parameter Journal of Aerosol Science 91, 43-53, 2016 DOI: 10.1016/j.jaerosci.2015.09.003

IPCC (2001) Climate Change 2001 - IPCC Third Assessment Report, the scientifc basis,chapter_5.2.2.1 Soil dust, Table 5.3 (available at https://www.ipcc.ch/ipccreports/tar/wg1/168.htm)

Iwasaka,Y., Shi, G.-Y.,Yamada, M., Matsuki, A., Trochkine, D., Kim,Y. S. et al. (2003). Importance of dust particles in the free troposphere over theTaklaman desert: Electron microscopic experiments of particles collected with a baloonborne particle impactor at Dunhunag, China. Journal of Geophysical Research, 108(D23), 8644.

Jaenicke, R. (1988). Aerosol Physics and Chemistry in Zahlenwerte und Funktionen aus Naturwissenschaft und Technik, Landolt Börnstein, Group 5 (Vol. 4, subvolume b), Physikalische und chemische Eigenschaften der Luft. Berlin, Germany: Springer.

Junge Ch. (1979) The importance of mineral dust as an atmospheric constituent. Chapter 2 of *Saharan Dust; mobilization, transport, deposition*. C. Morales, Ed.; John Wiley & Sons, pp. 49 - 60

Kandler K., Benker N., Bundke U.,Cuevas E., Ebert M.,, Knippertz E., Rodriguez S.,Schütz L., Weinbruch S., (2007) Chemical composition and complex refractive index of Saharan Mineral Dust at Izana, Tenerife (Spain) derived by electron microscopy. Atmospheric Environment 41 8058–8074

Kontratyev, K. Ya., Ivlev, L. S., Krapivin, V. F., & Varostos, C. A. (2006). Atmospheric aerosol properties. Formation, processes, impacts. Berlin: Springer, p. 141.

Mishchenko M.I., Hovenier J.W., Travis L.D. , Eds. (2000) Light scattering by nonsperical particles, theory, measurements and applications. Academic Press, 690 pp

Mishchenko, M. I., Travis, L. D., Kahn, R. A., & West, R. A. (1997). Modeling phase functions for dustlike tropospheric aerosols using a shape mixture of randomly oriented polydisperse spheroids. Journal of Geophysical Research, 102, 16831–16847.

Nousiainen T. and Kandler K. (2015) Light scattering by atmospheric mineral dust particles. In Light Scattering Reviews 9: Light Scattering and Radiative Transfer. A. Kokhanovsky, Ed. pp 3-52 Springer Praxis Books

Obregón M.A., Pereira S., Salgueiro V., Costa M.J,. Silva A.M, Serrano A., Bortoli D. Aerosol radiative effects during two desert dust events in August 2012 over the Southwestern Iberian Peninsula. Atmospheric Research, 2015; 153: 404 DOI: 10.1016/j.atmosres.2014.10.007

Von Hoyningen-Huene,W., & Posse, P. (1997). Nonsphericity of aerosol particles and their contribution to radiative forcing. Journal of Quantative Spectroscopy & Radiative Transfer, 57, 651–668.

Formatiert: Schriftart: Nicht Fett, Englisch (USA)

Formatiert: Schriftart: Nicht Fett

Formatiert: Schriftart: Nicht Fett, Englisch (USA)

Formatiert: Schriftart: Nicht Fett

Formatiert: Englisch (USA)

Formatiert: Englisch (USA)

Formatiert: Englisch (USA)

Formatiert: Englisch (USA)

Formatiert: Englisch (USA)

Formatiert: Englisch (USA)

Formatiert: Englisch (USA)

Valenzuela A., F. J. Olmo, H. Lyamani, M. Antón, A. Quirantes, and L. Alados-Arboledas (2012a) Aerosol radiative forcing during African desert dust events (2005–2010) over Southeastern Spain. Atmos. Chem. Phys., 12, 10331–10351

Valenzuela A., F. J. Olmo, H. Lyamani, M. Antón, A. Quirantes, and L. Alados-Arboledas (2012b) Classification of aerosol radiative properties during African desert dust intrusions over southeastern Spain by sector origins and cluster analysis. Journal of Geophysical Research 117 D06214 doi:10.1029/2011JD016885, 2012

Waldram, J. M. (1945). Measurement of the photometric properties of the upper atmosphere. Trans. Illum. Eng. Soc., 10, 147–188.

Xin, J.,Wang, S.,Wang,Y.,Yuan, J., Zhang,W., & Sun,Y. (2005). Optical properties and size distribution of dust aerosols over the Tengger Desert in Northern China. Atmospheric Environment, 39, 5971–5978.

Formatiert: Englisch (USA)

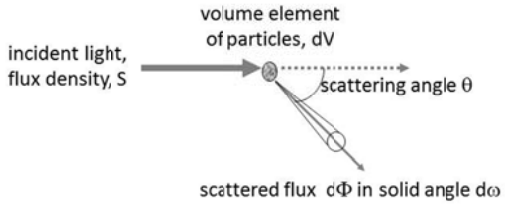

Figure 1: Definition of volume scattering function

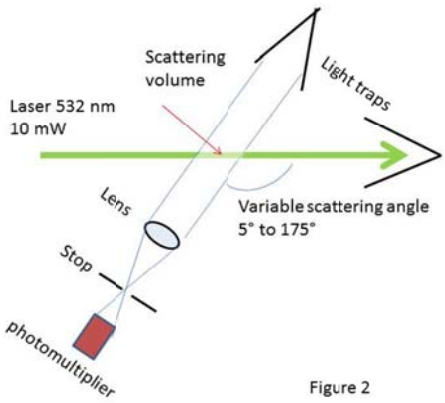

Figure 2: Principle of the polar nephelometer

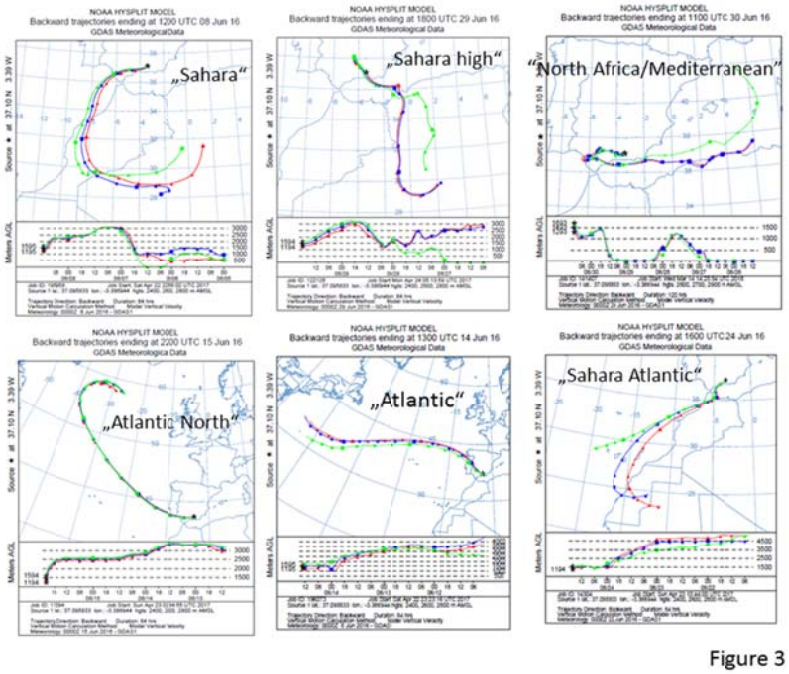

Figure 3: Back trajectories used for classification of aerosol types

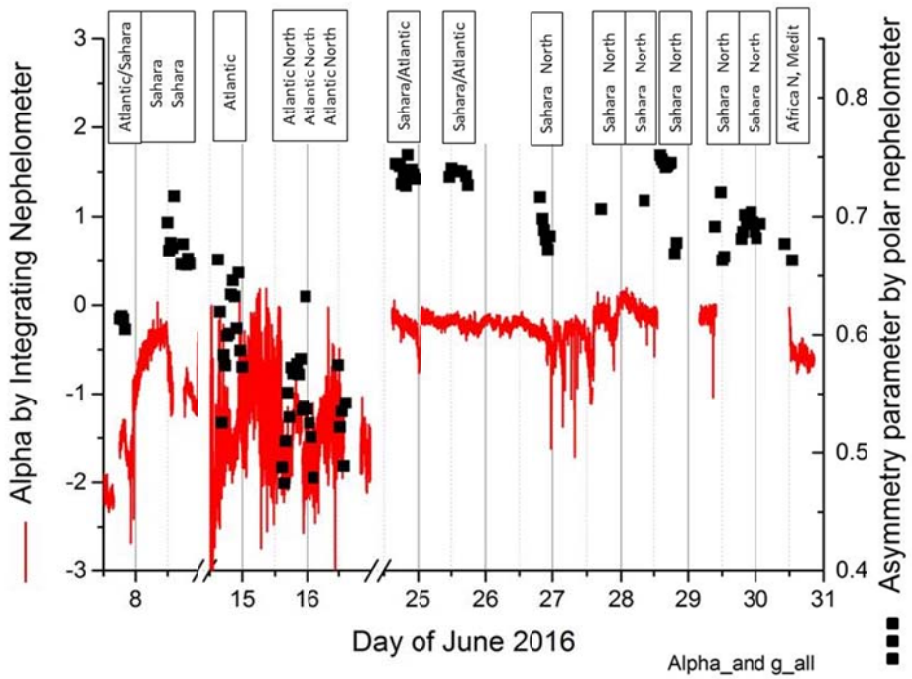

Figure 4: Angström exponent of the spectral scattering coefficient of the aerosol measured and classification by back trajectories. For the desert aerosol the Angström Exponent is larger than -1. In addition the asymmetry parameter is plotted too, for desert aerosol it is larger than 0.65.

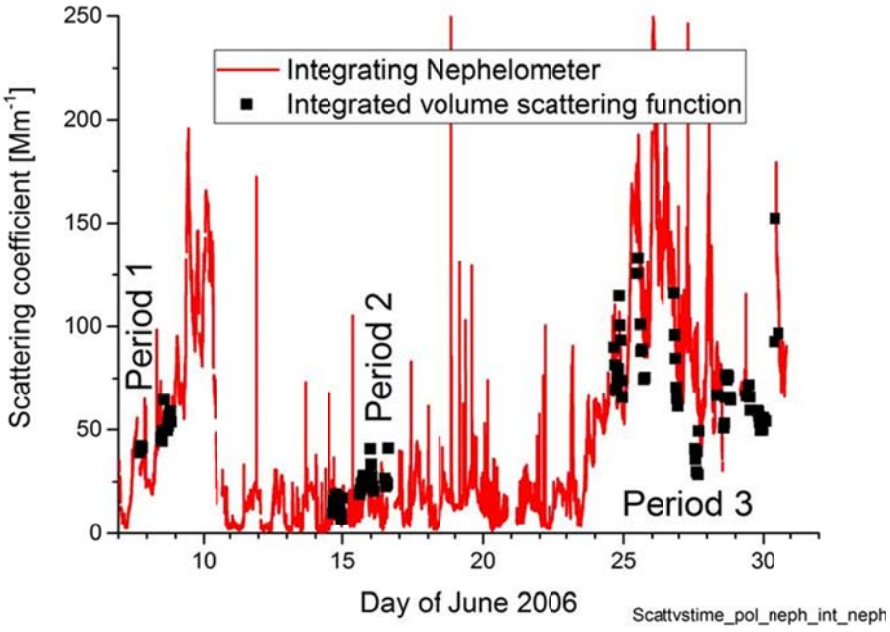

Figure 5: Measured scattering coefficient of the aerosol during the three periods of observation. The solid red line is the signal of the Integrating Nephelometer, the points are scattering coefficients obtained by integrating the measured volume scattering function.

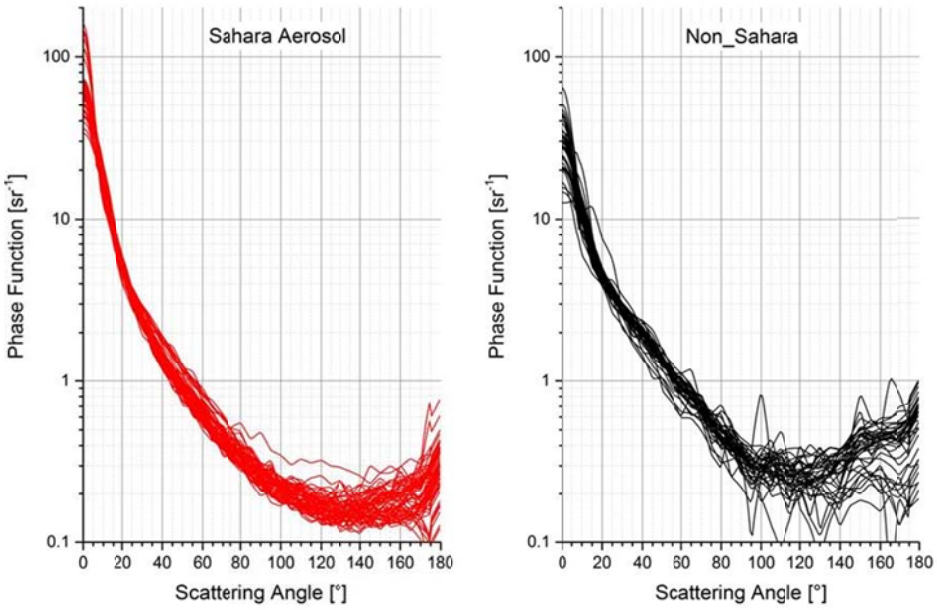

Figure 6. Comparison of phase function attributed to Sahara and non-Sahara aerosols.

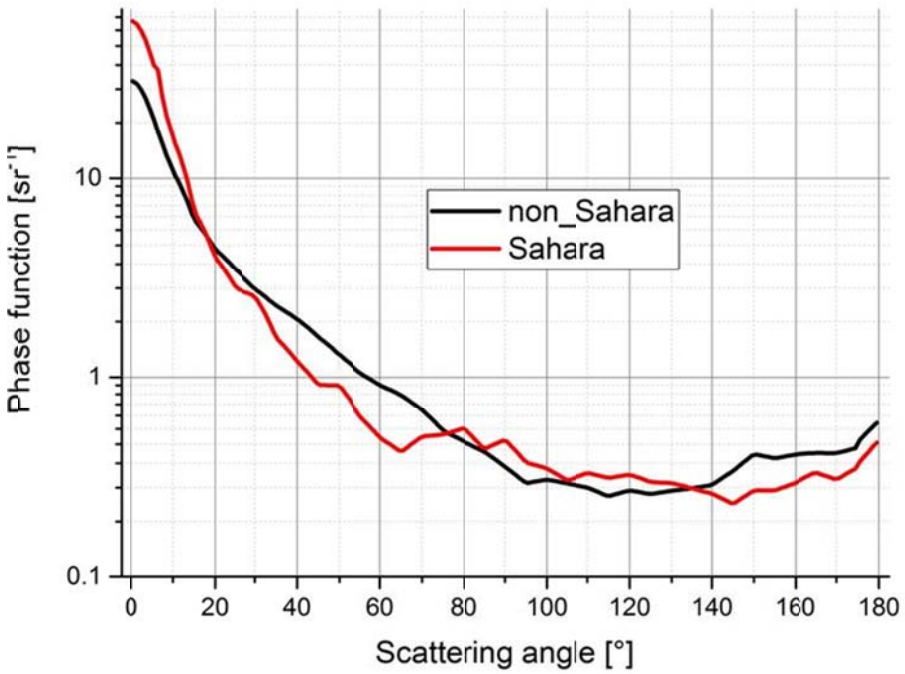
Phase function [sr⁻¹]
10
1
0.1
0
20
40
60
80
100
120
140
160
180
Scattering angle [°]
non_Sahara
Sahara

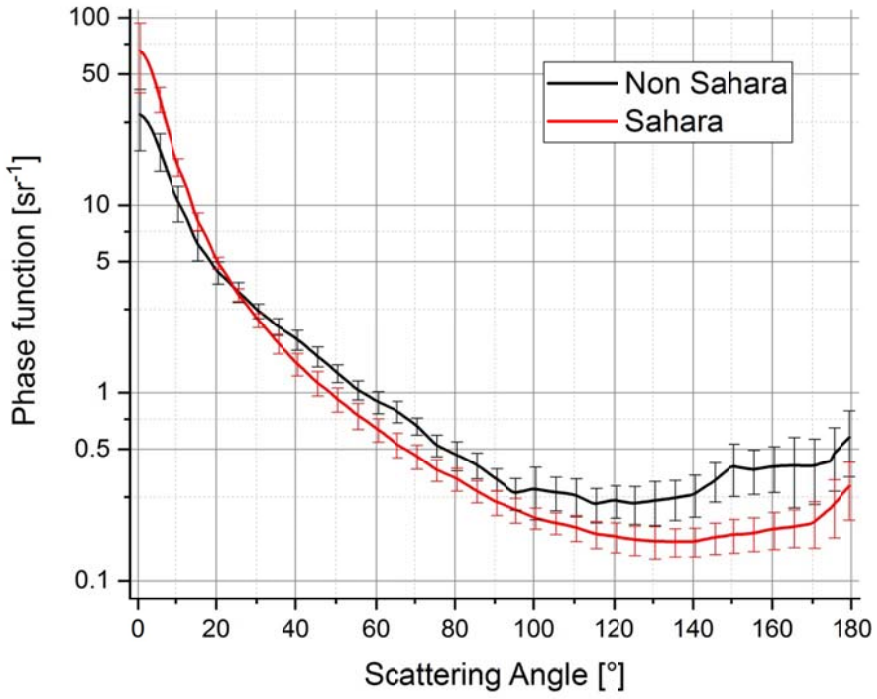

~~Figure~~ Figure 7. Average of the Sahara and non-Sahara aerosol phase functions.

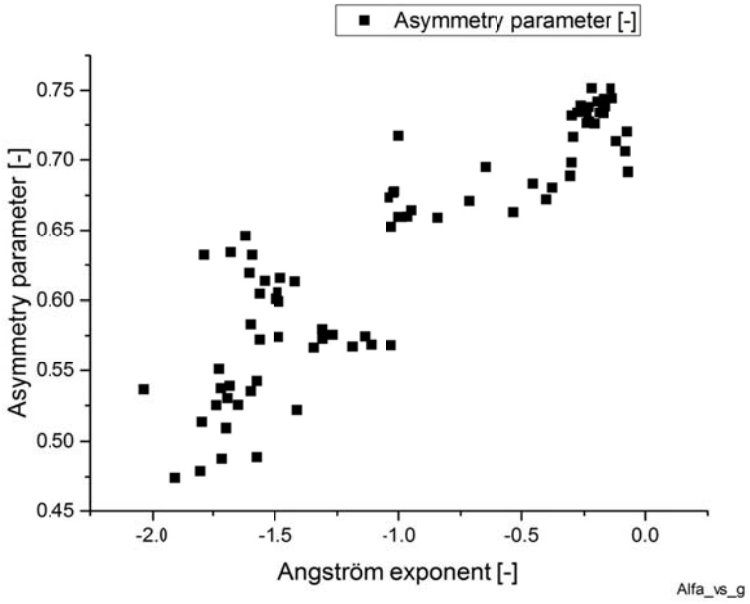

Figure 8. Relationship between the measured Angström exponent and the asymmetry parameter using the measured phase function.

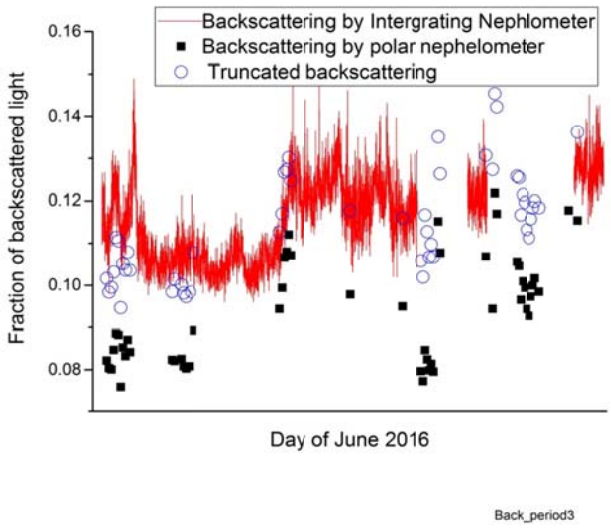

Figure 9. Back scattered fraction measured with the Integrating Nephelometer (red curve) and values obtained by the measured Volume scatteing function. Simulation of the truncation is shown by the hollow points.

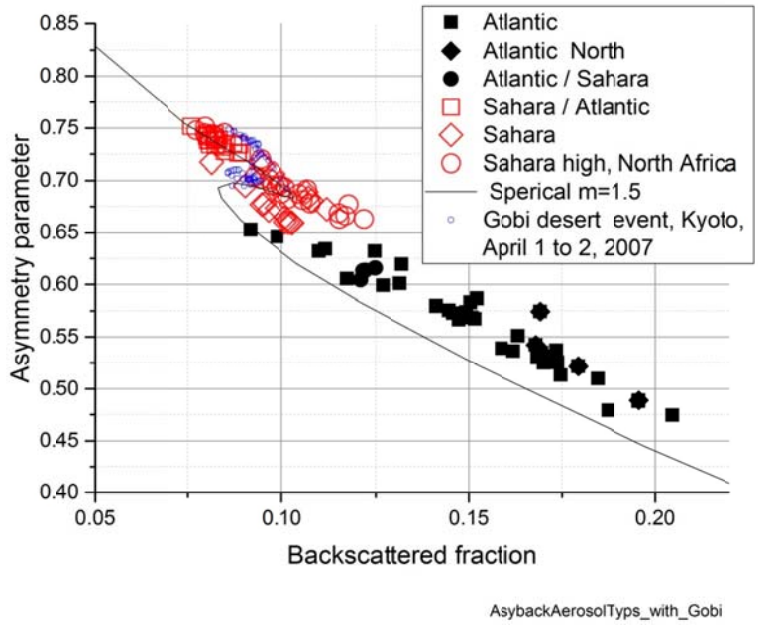

Figure 10: Asymmetry parameter and backscattered fraction calculated for the aerosols measured during this study. A clear separation between Sahara and non-Sahara aerosols is evident. The data points are in excellent agreement with data for the Gobi Desert aerosol.

Table 1. Classification of back trajectories		
Name	Air passes over	Remark
„Atlantic“	60°W<longitude<0°, 35°N<latitude<40°N	
“Atlantic North”	40°W<longitude<0°, 60°N<latitude<40°N	
“Sahara”	10°W<longitude<5°E,37°N<latitude<26°N	
“Sahara high”	5°W<longitude<5°E, 37°N<latitude<26°N	
“Sahara/Atlantic”, “Atlantic/Sahara” resp.	Up to 500 km West of the coast of Africa	Distinction between the two by Angström exponent
“North Africa/Mediterranean”	6°W<longitude<8°E, 35°N<latitude<37°	

5

Table 2. Characteristics of the two types of aerosols				
	Sahara aerosol		Non-Sahara Aerosol	
	Value	Stddev.	Value	Stddev.
Asymmetry parameter [-]	0.7106	0.032	0.562	0.0547
Backscattered fraction [-]	0.094	0.014	0.153	0.027
Average scattering coefficient [Mm^{-1}]	71	22	22.3	7.3
Phase function at 0° [sr^{-1}]	67	27	31	10
Phase function at 90° [sr^{-1}]	0.26	0.034	0.35	0.04
Phase function at 180° [sr^{-1}]	0.31	0.11	0.59	0.21
Lidar ratio [sr^{-1}]	44	16	23	8